Modeling of a Double Effect Heat Transformer Operating with Water/Lithium Bromide

Authors:

Itzel N. Balderas-Sánchez, J. Camilo Jiménez-García, Wilfrido Rivera

Date Submitted: 2019-08-14

Keywords: COP enhancement, water-lithium bromide, thermal energy upgrade, absorption heat transformer

Abstract:

Absorption heat transformers are effective systems for a wide variety of applications; however, their main purpose is to upgrade thermal energy from several sources at low-temperature up to a higher temperature level. In the literature, several advanced configurations for absorption heat transformers have been reported which are mainly focused on the improvement of the gross temperature lift by the use of a double absorption process; however, these systems usually offer a reduced coefficient of performance. The present study proposes a new advanced configuration of an absorption heat transformer that improves the coefficient of performance utilizing a double generation process. The operation of the new configuration was numerically modeled, and the main findings were discussed and presented emphasizing the effect of several parameters on the system performance. The highest coefficient of performance and gross temperature lift were 0.63 and 48 °C, respectively. From its comparison with a single-stage heat transformer, it is concluded that the proposed system may achieve coefficient of performance values up to 25.8% higher than those obtained with the single-stage system, although achieving lower gross temperature lifts.

Record Type: Published Article

Submitted To: LAPSE (Living Archive for Process Systems Engineering)

Citation (overall record, always the latest version):	LAPSE:2019.0949
Citation (this specific file, latest version):	LAPSE:2019.0949-1
Citation (this specific file, this version):	LAPSE:2019.0949-1v1

DOI of Published Version: https://doi.org/10.3390/pr7060371

processes

MDPI

Article

Modeling of a Double Effect Heat Transformer Operating with Water/Lithium Bromide

Itzel N. Balderas-Sánchez, J. Camilo Jiménez-García and Wilfrido Rivera *

Instituto de Energías Renovables, Universidad Nacional Autónoma de México, Temixco 62580, Mexico; inbas@ier.unam.mx (I.N.B.-S.); jcjig@ier.unam.mx (J.C.J.-G.)

* Correspondence: wrgf@ier.unam.mx; Tel.: +52-5556229740

Received: 17 May 2019; Accepted: 8 June 2019; Published: 14 June 2019

Abstract: Absorption heat transformers are effective systems for a wide variety of applications; however, their main purpose is to upgrade thermal energy from several sources at low-temperature up to a higher temperature level. In the literature, several advanced configurations for absorption heat transformers have been reported which are mainly focused on the improvement of the gross temperature lift by the use of a double absorption process; however, these systems usually offer a reduced coefficient of performance. The present study proposes a new advanced configuration of an absorption heat transformer that improves the coefficient of performance utilizing a double generation process. The operation of the new configuration was numerically modeled, and the main findings were discussed and presented emphasizing the effect of several parameters on the system performance. The highest coefficient of performance and gross temperature lift were 0.63 and 48 °C, respectively. From its comparison with a single-stage heat transformer, it is concluded that the proposed system may achieve coefficient of performance values up to 25.8% higher than those obtained with the single-stage system, although achieving lower gross temperature lifts.

Keywords: absorption heat transformer; thermal energy upgrade; water-lithium bromide; COP enhancement

1. Introduction

In the last decades, the utilization of absorption heat transformers (AHT) has been the focus of attention of engineers and scientists, mainly due to the high potential that this kind of systems offer to upgrade thermal energy from a low-temperature source up to a higher temperature level for several practical purposes, at a relatively low cost. The characteristics of AHT make its use very attractive when geothermal or solar energy sources are used as heat input, or even by using industrial waste heat.

Three review papers have been published on the research of AHT, which were realized by Parham et al. [1], Donnellan et al. [2] and Rivera et al. [3]. These three papers summarized some of the applications of theoretical and experimental systems working with different mixtures. The papers cited below are some of the most outstanding investigations about advanced configurations found in the literature.

1.1. Theoretical Investigations about Advanced Heat Transformers

The majority of the investigations available in the literature on advanced absorption heat transformers are numerical studies with different purposes, but in general, they seek to identify the thermodynamic limits and performance of each proposed configuration. Rivera et al. [4,5] published two investigations to evaluate the effect of the heat exchangers on advanced heat transformers. It was found that increasing the effectiveness of the economizer improved the performance of the system when the temperature of the absorber was at least 40 °C above the temperature of the heat source. Also, a

comparison between the single and two-stage configurations was presented. Besides, the authors found that higher gross temperature lifts (GTL) could be obtained with the double-stage heat transformers, although with lower coefficients of performance. Ji and Ishida [6] proposed a series of modifications to the double-stage cycle using energy utilization diagrams and modes of sensible and latent heat exchange in the generators and absorbers. These changes allowed to obtain GTL values higher than 10.7 °C and increments in exergy efficiency close to 7%, although the coefficient of performance (COP) had a slight decrease.

In 2002, Göktun and Er [7] used an irreversible thermodynamic approach to investigate the optimal performance of a cascade absorption heat transformer. In this study, the authors took into account the internal irreversibilities as well as the thermal resistances, whose effects were considered in the equation to calculate the COP. It was found that the cascade system achieved a significant increase in GTL (9%) with respect to the single-stage cycle.

Zhao et al. [8,9] proposed a novel configuration for a double absorption cycle and a new solution cycle, respectively. From a comparison with similar configurations, it was found that the proposed cycle was able to achieve better COP at high absorption temperatures, reaching a maximum value of 0.32. The gross temperature lifts varied from 60–100 °C.

Some numerical simulations were carried out by Rivera et al. [10] to analyze the performance of heat transformers coupled with solar ponds. The objective of the investigation was to obtain the highest temperature of the useful heat. The single-stage and double-absorption configurations were found to offer the best results, with the former, it was found that it was possible to increase the temperature of the pond up to 50 °C with a COP close to 0.48; while with the latest configuration, the temperature of the pond could be increased up to 100 °C with a COP of 0.33.

Lee and Sherif [11] studied the thermodynamic behavior of a triple-absorption heat transformer. The authors found that the GTL was higher than that obtained with single-stage and double-absorption heat transformers (DAHT), although the values for the COP were lower than those obtained with the other systems. It was found that the COP increased with the temperature of the heat source and decreased with an increment of the condensation temperature.

Donnellan et al. [12] investigated the optimal number and location of the internal heat exchangers in a triple-absorption heat transformer. The authors found that in the conventional configuration, the heat exchangers were not used effectively, in such a way that the COP could be increased by 11.7%, and the irreversibilities could be reduced by 21%. Later Donnellan et al. [13], determined the main factors affecting the performance of the system, finding that the condenser temperature and the heat transfer gradient had the most important effect. This study also demonstrated that the maximum exergy destruction takes place in the generator, followed by the two absorber-evaporators.

Regarding exergy destruction, Fartaj [14] and Martínez and Rivera [15] analyzed a DAHT using the first and second law of thermodynamics. The authors found that the maximum exergy destruction occurred in the generator. Moreover, it was proved that the performance of the system is better when the temperatures of the generator, evaporator, and evaporator-absorber increased, and the temperatures of the absorber and the condenser decreased. These results were consistent with those reported by Wang et al. [16] who showed that in the generator, condenser, and absorber-evaporator, occurred the most of exergy destruction.

In other investigations, Wang et al. [17] introduced a new double-absorption heat transformer able to reach a maximum COP value of 0.33 when the temperature of the absorber was 130 °C, the evaporator and generator temperatures were 80 °C, the absorber-evaporator was 105 °C, and the condenser temperature was 30 °C. On the other hand, Liu et al. [18] proposed a heat transformer (HT) able to operate at absorption powers from 7.2–15.5 kW, obtaining COP values from 0.2–0.38. The maximum absorption temperature achieved was 124 °C, while the maximum GTL reached was 34.8 °C.

Recently, Salehi et al. [19] studied the crystallization risk of the H_2O-LiBr mixture under different operating conditions in several components in single, double, and triple-effect heat transformers. It was found that high absorber temperatures increased the risk of crystallization at the outlet of the

expansion valves, particularly in the case of double and triple-effect systems. Moreover, it was proved that in any of the configurations analyzed, low condensation temperatures, together with low heat exchanger efficiencies, increased the crystallization risk.

On the other hand, Hernández-Magallanes et al. [20] proposed a new cycle integrating a heat transformer with a heat pump capable of producing electric power and useful heat, simultaneously. This cycle was modeled considering its operation with the working pair NH_3-$LiNO_3$. The simulations showed that it was possible to obtain increases in the temperature of the supplied heat up to 40 °C, and, at the same time, to produce 300 kW of electric power. Also, from the comparison of this cycle with an Organic Rankine Cycle (ORC) and a HT, operating separately at the same temperature conditions, it was demonstrated that the proposed cycle could reduce the energy usage and the irreversibilities by 32.3% and 21.6%, respectively.

1.2. Experimental Investigations

The majority of the experimental investigations found in the literature, analyze the performance of single-stage heat transformers (SSHT), and some of the most relevant studies are the following: Rivera et al. [21] analyzed the performance of an experimental single-stage heat transformer, based on the first and second laws of thermodynamics. From the results, it was determined that the best COP of the system was obtained at higher solution concentrations; the contrary occurred when the temperature of the absorber was increased. Also, it was noticed that the absorber contributed with about half of the system irreversibilities. To reduce these irreversibilities, Colorado et al. [22] proposed a methodology based on neural networks, by which the irreversibilities could be reduced up to 14%.

In another work, Rivera et al. [23] utilized some additives to increase the heat transfer coefficient in the absorber and generator of a SSHT, decreasing with their use the irreversibilities and improving the system performance. The authors reported that the absorption temperatures were increased by 5 °C by adding 400 ppm of 2-ethyl-1-hexanol, while the COP increased up to 40%, being the highest COP value close to 0.49.

On the other hand, as an alternative method to improve the corrosion resistance capacity in the materials used as components of heat transformers, mainly operating with the H_2O-LiBr mixture, Oloarte et al. [24] proposed the introduction of graphite disks arranged in a column inside the absorber. The results of this investigation demonstrated that the heat transfer coefficients could be increased by this method. Also, Márquez-Nolasco et al. [25] also studied the utilization of graphite disks in components of a heat transformer. The authors evaluated a generator with 18 graphite disks. The COP registered varied from 0.25–0.48.

Ma et al. [26] assessed an experimental AHT with the vapor absorption taking place inside vertical spiral tubes. It was demonstrated that the coefficient of performance and thermal efficiency decreased when the solution flow increased. Also, it was proved that the influence of the hot water mass flow rate on the performance of the system is negligible. The maximum COP reported was 0.4.

More recently, in Korea, Hong et al. [27] analyzed the possibility of generating steam by the use of a SSHT. In their research, the authors suggested a couple of modes to supply the heat load to the system. According to the results, the operation mode depends on the effect desired, having the choice to maximize the steam production or the COP.

On the other hand, Conde et al. [28] studied the conditions to optimize the performance of a heat transformer with energy recycling. It was found that the generation temperature is one of the main variables to pay attention when it is desired to increase the COP and get energy savings.

From the literature reviewed, it can be verified that the majority of the advanced configurations of heat transformers reported in the literature are mainly focused on getting high gross temperature lifts for different purposes. It also can be noticed that although several papers proposed to improve the performance of these systems by the enhancement of the coefficient of performance or by any other method, none of the papers in the literature proposed a double-generation or also called double-effect process (by similarity with absorption cooling systems) to increase the coefficient of performance. In the

present study, a new configuration of an advanced absorption heat transformer called double-effect heat transformer (DEHT) operating with the water/lithium bromide mixture is analyzed.

2. System Description

2.1. Single-Stage Heat Transformer

The main objective of the SSHT is to use waste heat or renewable energies such as solar thermal or geothermal energy, to transform it into useful heat at a higher temperature level.

The diagram of the SSHT is shown in Figure 1. The principal components of the system are an evaporator, an absorber, a generator, a condenser, and an economizer. Its operating principle is as follows: the liquid-phase mixture enters to the generator, where a determined amount of heat is supplied at a generation temperature (T_G) to evaporate part of the working fluid from the absorbent. The vaporized working fluid leaving the generator (point 1) enters to the condenser where a quantity of heat is delivered at the condenser temperature (T_C) from the working fluid condensation, which leaves the component in saturated conditions (point 2). Then, the working fluid is pumped to the evaporator incrementing its pressure (point 3). In the evaporator, an amount of heat is supplied at an evaporator temperature (T_E) to produce vapor at saturated conditions (point 4). In the absorber, the vapor is absorbed by the solution with high absorber concentration leaving the generator (point 8) delivering an amount of useful heat at the absorber temperature (T_A), being this the highest system temperature. The weak solution leaving the absorber (point 5) flows through the economizer (point 6) preheating the solution going from the pump (point 9) to the absorber (point 10). Finally, the solution leaving the economizer passes through the valve, reducing its pressure (point 7) before entering the generator, starting the cycle again.

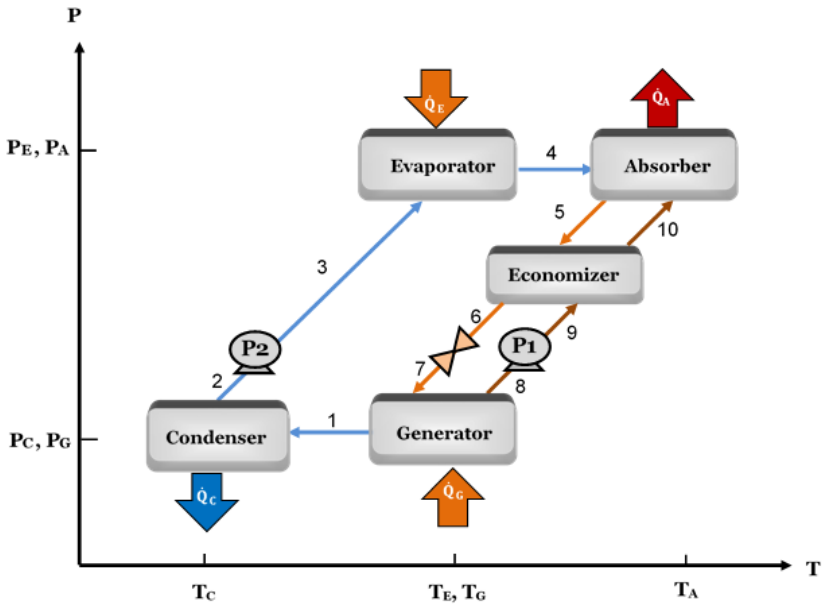

Figure 1. Temperature and pressure levels of a single-stage heat transformer (SSHT).

According to Figure 1, the system operates at two pressure levels and three temperature levels. It is considering that the heat is supplied at the same temperature to the evaporator and the generator.

2.2. Double-Effect Heat Transformer

As can be seen in Figure 2, in the DEHT an extra heat exchanger called generator/condenser is added to the system which has a double purpose. One side of the heat exchanger acts as a condenser condensing the working fluid produced in the generator, while the other side acts as a second generator

which produces a second stream of refrigerant by using the heat delivered from the condensation process of the working fluid. So, in this way, with the proposed system it is possible to produce a second amount of working fluid by supplying heat at intermediate temperature to only one generator and the evaporator, in a similar way that the single-state heat transformer. It is important to mention that in this system the heat supplied to the generator must be at a higher temperature level than the heat supplied to the generator in the SSHT in order that the second generation process can produce refrigerant. The rest of the DEHT operates similarly than the SSHT described in Section 2.1.

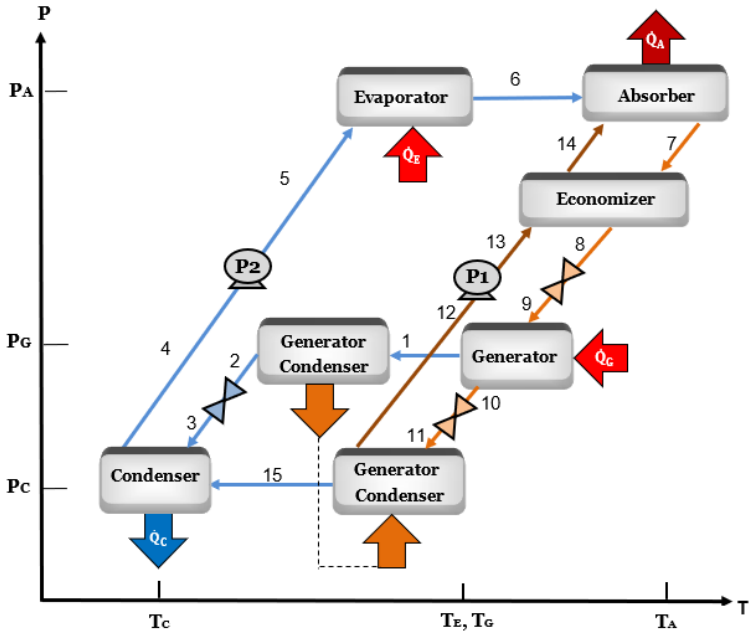

Figure 2. Temperature and pressure levels of a double-effect heat transformer (DEHT).

3. Mathematical Model

The modeling of the cycle considered energy, mass, and matter balances in each component of the system. The simulation was performed in the Engineering Equation Solver (EES) (Academic Professional V10.464-3, F-Chart Software, WI, U.S.)

3.1. Assumptions

For the heat transformer analysis, the following assumptions were adopted in the development of the mathematical model:

i. In order to calculate the properties of the system, thermodynamic equilibrium conditions are considered.
ii. The cycle works in steady-state conditions.
iii. A rectifier is not required since there is not absorbent evaporation throughout the cycle.
iv. The same source is used to supply the heat to both the generator and the evaporator.
v. Heat losses from the heat transformer components are considered negligible.
vi. Refrigerant saturation points are assumed at the exit of the condenser, the evaporator, and the generator/condenser.
vii. Saturation conditions for the solution are assumed at the exit of the absorber, the generator, and the generator/condenser.
viii. Pressure losses due to friction are neglected.
ix. The pumping process is isentropic.
x. The throttling process in the valves is isenthalpic.

3.2. Main Equations

The main equations used for the simulation of the DEHT are presented in Table 1. This table shows the heat loads in the condenser ($\dot{Q}_C$), the absorber ($\dot{Q}_A$), the evaporator ($\dot{Q}_E$), the generator ($\dot{Q}_G$), and the generator/condenser ($\dot{Q}_{GC}$), the works done by pump 1 ($\dot{W}_{P1}$), and the pump 2 ($\dot{W}_{P2}$), the GTL, the COP, the economizer effectiveness (η_{EC}) and the exergy efficiency (η_{EX}). T_0 in the exergy equation represents the ambient temperature.

The SSHT was modeled using similar equations and algorithm as the DEHT. The expressions utilized to calculate the coefficient of performance, the gross temperature lift, and the exergy coefficient of performance are reported by Rivera et al. [21]. The economizer effectiveness is defined as the ratio between the actual heat transfer to the maximum possible heat that could be transferred. To determine this value, the lowest enthalpy must be calculated according to Ibarra et al. [29], this enthalpy is $h_{7,13}$ (at a concentration 7 and temperature 13).

Table 1. Main equations for the double-effect heat transformer (DEHT).

Double Effect Heat Transformer	
Absorber (A)	**Condenser (C)**
$\dot{m}_6 + \dot{m}_{14} = \dot{m}_7$	$\dot{m}_3 + \dot{m}_{15} = \dot{m}_4$
$\dot{m}_6\, X_6 + \dot{m}_{14} X_{14} = \dot{m}_7 X_7$	$\dot{m}_3 h_3 + \dot{m}_{15} h_{15} = \dot{m}_4 h_4 + \dot{Q}_C$
$\dot{m}_6\, h_6 + \dot{m}_{14} h_{14} = \dot{m}_7 h_7 + \dot{Q}_A$	**Economizer (EC)**
Evaporator (E)	$\dot{m}_7 h_7 + \dot{m}_{13} h_{13} = \dot{m}_8 h_8 + \dot{m}_{14} h_{14}$
$\dot{m}_5 h_5 + \dot{Q}_E = \dot{m}_6 h_6$	$\eta_{EC} = (h_{14} - h_{13}) / \left(h_7 - h_{7,13}\right)$
Generator (G)	**Coefficient of Performance (COP)**
$\dot{m}_9 = \dot{m}_1 + \dot{m}_{10}$	$COP = \dot{Q}_A / (\dot{Q}_E + \dot{Q}_G + \dot{W}_{P1} + \dot{W}_{P2})$
$\dot{m}_9 X_9 = \dot{m}_1 X_1 + \dot{m}_{10} X_{10}$	**Gross Temperature Lift (GTL)**
$\dot{m}_9 h_9 + \dot{Q}_G = \dot{m}_1 h_1 + \dot{m}_8 h_8$	$GTL = T_A - T_G$
Generator-Condenser (GC)	**Flow Ratio (FR)**
$\dot{m}_{11} = \dot{m}_{12} + \dot{m}_{15}$	$FR = \dot{m}_7 / \dot{m}_4$
$\dot{m}_{11} X_{11} = \dot{m}_{12} X_{12} + \dot{m}_{15} X_{15}$	**Exergy Efficiency**
$\dot{m}_{11} h_{11} + \dot{Q}_{GC} = \dot{m}_{12} h_{12} + \dot{m}_{15} h_{15}$	$\eta_{EX} = \frac{\dot{Q}_A\left(1 - \frac{T_0}{T_A}\right)}{\dot{Q}_G\left(1 - \frac{T_0}{T_G}\right) + \dot{Q}_E\left(1 - \frac{T_0}{T_E}\right) + \dot{W}_{P1} + \dot{W}_{P2}}$
$\dot{m}_1 h_1 = \dot{m}_2 h_2 + \dot{Q}_{GC}$	

3.3. Input Data

The input data for the development of the mathematical model is shown in Table 2. The range of condensation temperature is between 20 °C and 40 °C. The effectiveness of the economizer was set in 0.8 and the thermal absorption power in 10 kW, for the base case. The generation temperature varied between 70–130 °C (simulating the waste heat supplied by an industrial process); however, for the SSHT the highest T_G was set on 100 °C since this system cannot operate at higher temperatures due to crystallization problems. The absorption temperature varied from 100 °C up to the maximum possible value that each cycle can reach. Finally, T_{GC} was between 50–100 °C, which is an intermediate temperature between the condenser and the generator.

Table 2. Input data.

	SSHT	**DEHT**	
Variable	**Operation Range**		**Increment**
T_C (°C)	20–40		5
T_A (°C)	100–170	100–194	2
T_G (°C)	70–100	75–130	5
T_{GC} (°C)	-	50–100	1
η_{EC}	0.8		-
$\dot{Q}_A$ (kW)	10		-

3.4. Algorithm

The algorithm followed for the simulation of the DEHT is shown in Figure 3. The input parameters were: The useful power produced in the absorber, the economizer effectiveness, and the temperatures of generation ($T_G = T_1$), generation/condensation, ($T_{GC} = T_2$), condensation ($T_C = T_4$), and absorption ($T_A = T_9$).

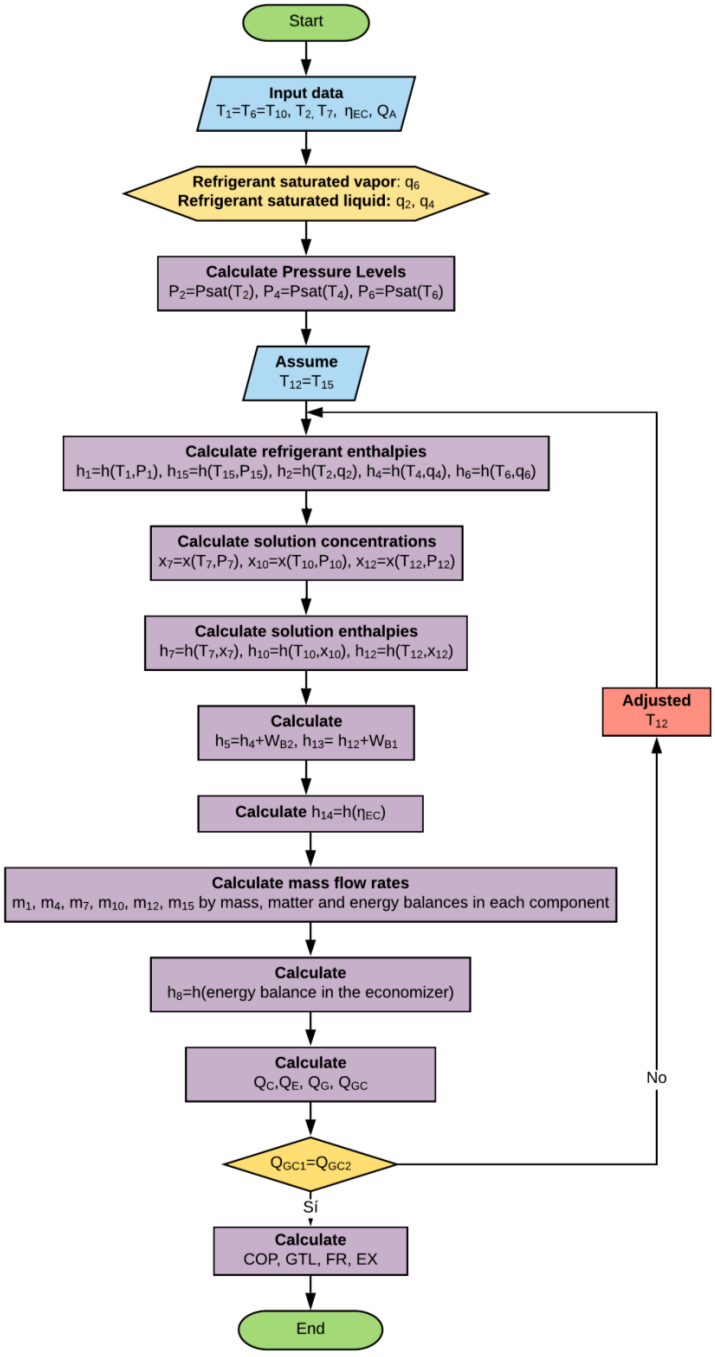

Figure 3. Algorithm flow chart for the modeling of the DEHT.

4. Results

4.1. Modeling of the DEHT

Figure 4 presents the coefficients of performance as a function of T_A for different values of T_G. In this figure, it can be observed that the COP values decrease rapidly with the increment of T_A. This behavior is expected, since the increment of T_A also causes an increment on the concentration of the solution leaving the absorber, thus reducing the concentration difference between the two solutions flowing from the generator to the absorber and from the absorber to the generator. The decrease in concentrations causes that the system loses the ability to generate and to absorb the working fluid, thus reducing the coefficients of performance. Also, it can be seen that the absorber temperatures achieved by the system strongly depend on the values of T_G.

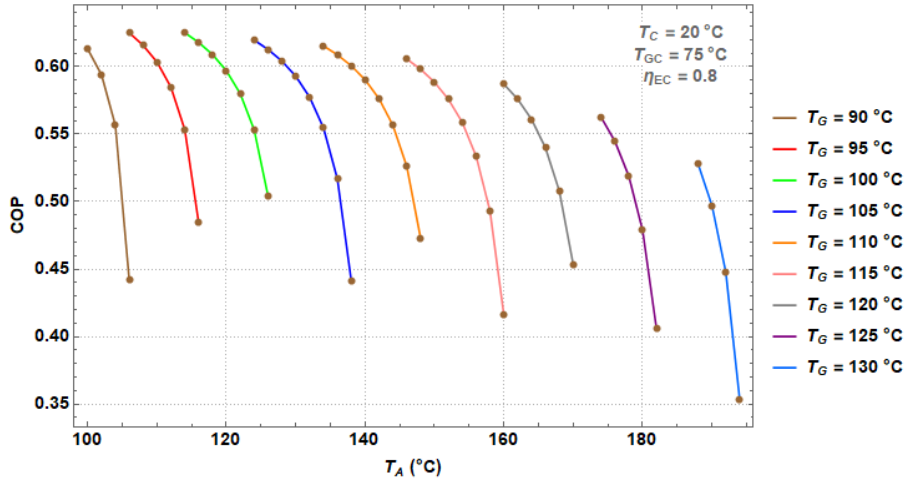

Figure 4. COP as a function of T_A at different T_G values for the DEHT.

Figure 5 shows the COP as a function of the GTL for different T_C values. From this figure, it can be observed that the COP decreases with an increment of the gross temperature lift. This behavior occurs for the same reasons explained in Figure 4, since the GTL is defined as the difference between T_A and T_G. From the figure, it can be seen that the maximum COP are higher 0.6 for gross temperature lifts of 25 °C, while the lowest coefficients of performance are about 0.4 for gross temperature lifts of 40 °C. Besides, it can be observed that the COP decreases with an increment of the T_C values. The increase in T_C causes the system to dissipate heat at a higher temperature, which causes a decrease in the COP.

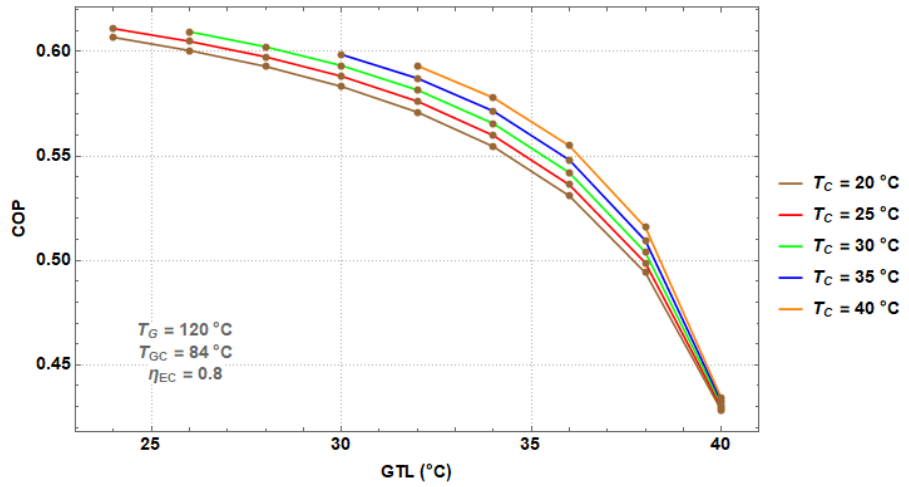

Figure 5. COP as a function of GTL at different T_C values for the DEHT.

Figure 6 shows the COP as a function of T_G for different T_C values. It can be observed that the COP increases significantly with an increase of T_G, augmenting from 0.46 at a T_G value of 85 °C, up to 0.62, at a T_G of 105 °C. The increment of the coefficient of performance occurs due to the higher amount of the working fluid produced by the increment of the temperature of the heat supplied to the component.

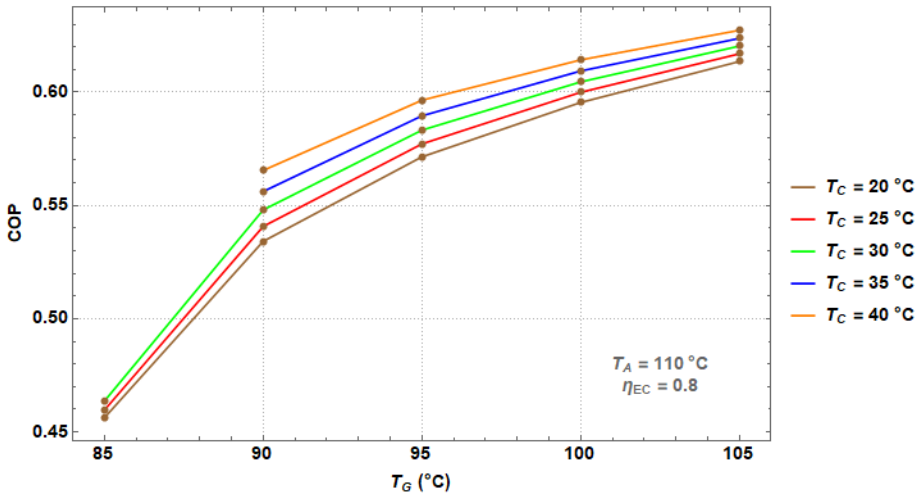

Figure 6. COP as a function of T_G at different T_C values for the DEHT.

Figure 7 shows the variation of the COP as a function of the flow ratio. It can be seen that the flow ratio is a critical variable in the system performance since the coefficient of performance rapidly decreases with the increment of this parameter. This behavior is justified by the flow ratio definition, since an increment of the flow ratio means that the amount of the working fluid decreases with respect to the solution flowing from the generator to the absorber, causing that a higher amount of energy has to be supplied to the generator, thus reducing the coefficient of performance. Besides, the COP decreases with an increment of T_C for the reasons explained in Figure 5.

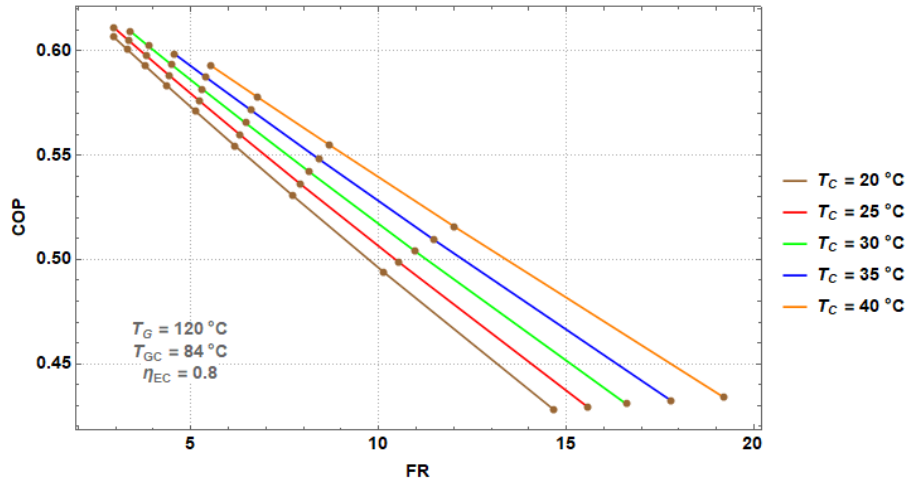

Figure 7. COP as a function of FR at different T_C values for the DEHT.

Figure 8 presents the variation of the COP as a function of the economizer effectiveness at different generation temperatures. It can be observed that at higher T_G, the value of the economizer effectiveness practically does not affect the coefficient of performance, since for a T_G = 110 °C, the COP goes from 0.593 to 0.608 for effectiveness values of 0.5 and 0.9, respectively. However, at lower T_G values, such as T_G = 90 °C, the economizer effectiveness is very important since the coefficient of performance raises

from 0.31 up to 0.5 for economizer effectiveness of 0.5 and 0.9, respectively. This behavior occurs since an increase in T_G, causes an increment in the solution temperature leaving the generator/condenser (T_{12}), thus reducing the heat transfer potential since T_{12} gets closer to the absorber temperature (T_7) which remains constant; however, at low T_G values the difference between T_7 and T_{12} becomes higher, increasing the heat recovered in the economizer, thus increasing the COP.

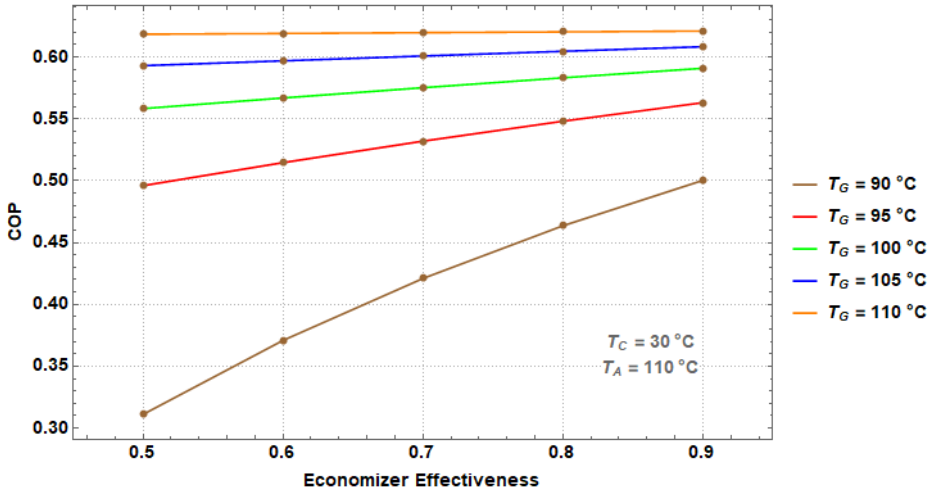

Figure 8. COP as a function of the economizer effectiveness at different T_G values for the DEHT.

Figure 9 shows the exergy efficiency as a function of the T_G for different T_C values. It can be seen that the exergy increases significantly with an increase of T_G, the minimum exergy value achieved is around 0.5 at a T_G of 85 °C, and the maximum values are around 0.62 at a T_G of 105 °C. Besides, the exergy efficiency increases when T_C increases due to the reasons explained in Figure 6.

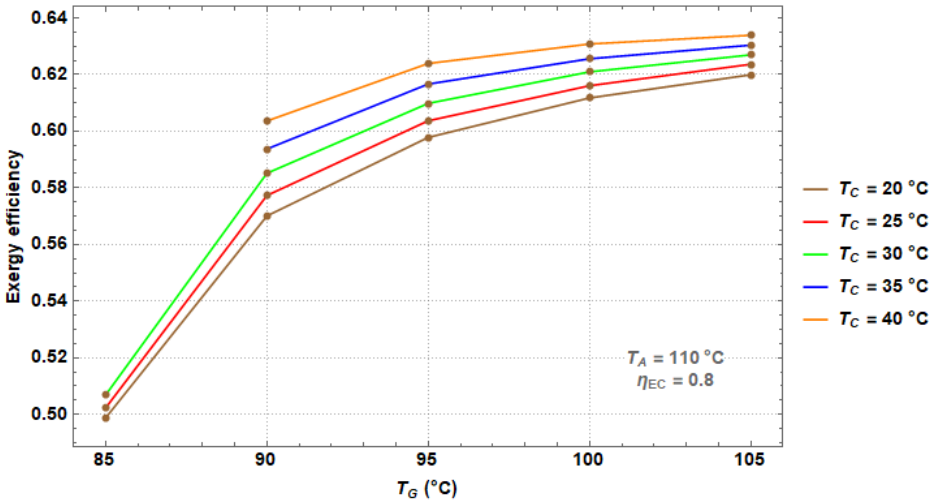

Figure 9. Exergy as a function of the T_G for different T_C values for the DEHT.

4.2. Comparison of the Performance between the SSHT and the DEHT

In order to show the advantages and disadvantages of the DEHT with respect to the SSHT, Figures 10–12 compare the COP, the GTL, and the exergy efficiency, respectively.

Figure 10 shows the variation of the COP with respect to the generation temperature, at a condensation temperature of 30 °C, for the two heat transformer configurations. As can be seen, the systems operate at different ranges of T_G. The SSHT operates at T_G between 70 °C and 85 °C, while the DEHT operates at T_G between 85 °C and 105 °C. For the SSHT, the COP values slightly vary with

the increment of T_G, from approximately 0.45–0.49, while the DEHT achieves higher COP values from 0.46–0.62, which represents an increment of 25.8% with respect to those values obtained with the SSHT, for these specified conditions. Besides, it can be seen that the COP increases with the increment of T_G, as it was previously explained in Figure 6.

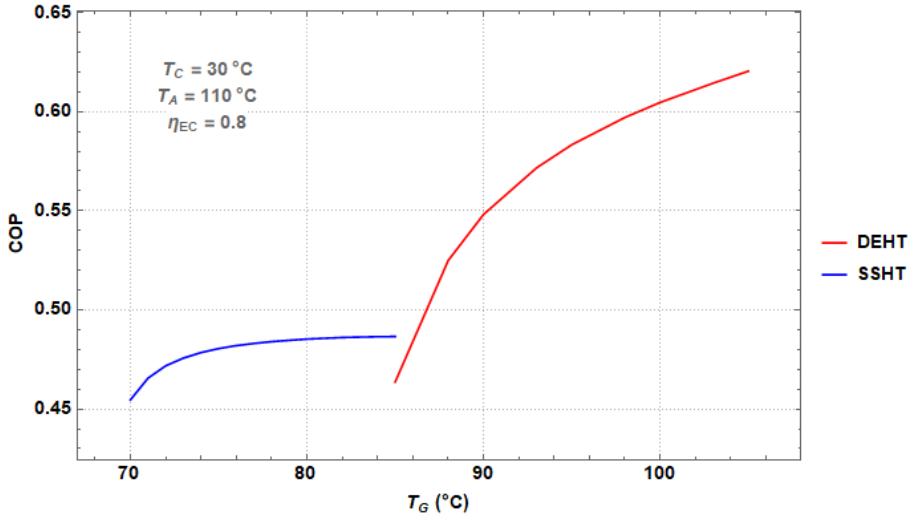

Figure 10. Comparison of the COP as a function of T_G for the two different heat transformers.

Figure 11 compares the COP as a function of the GTL for both systems. As it was seen in Figure 10, the SSHT and DEHT operate at different generation temperatures, which are specified for each system in Figure 11. As it can be observed, the COP values remain almost constant for the SSHT at gross temperature lifts up to 50 °C, and then rapidly decrease to a minimum value of 0.27 at a GTL of 63 °C. On the other hand, the COP rapidly decreases for the DEHT with the increment of GTL, achieving a maximum GTL of 48 °C. Despite this disadvantage, it can be observed that with the DEHT, it is possible to achieve higher COP values than those obtained with the SSHT up to GTL values of 45 °C.

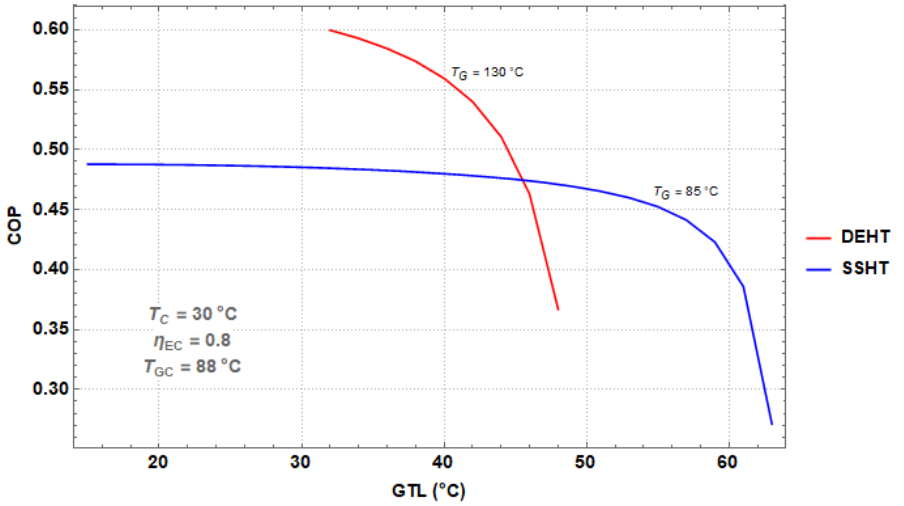

Figure 11. Comparison of the COP as a function of the GTL for the two different heat transformers.

Figure 12 compares the exergy efficiency for both systems as a function of T_A. Since the SSHT may operate at temperatures from 85 °C, it can be seen exergy values for T_A varying from 100 °C to 146 °C, while for the DEHT the exergy efficiency is reported for T_A varying from 161 °C–175 °C. This happens since, for the specified conditions, the generation temperature is considerably higher with the DEHT than with the SSHT. For the DEHT the maximum exergy efficiency was 0.62, while for the SSHT

the maximum exergy was 0.54. These values are in concordance with the COP values reported for both systems in Figure 10.

From the comparison presented for both systems, it is possible to observe that the SSHT can operate at generation temperatures from 70 °C, can achieve GTL values up to 63 °C and can deliver useful heat at absorber temperatures of 148 °C, obtaining a maximum COP value of 0.48. On the other hand, the proposed system has the disadvantages of requiring generator temperatures of a least 85 °C, reaching a maximum GTL value of 48 °C. Nevertheless, the proposed system can achieve COP values as high as 0.63, which is 25.8% higher than those achieved with the SSHT. Besides, the DEHT can deliver useful heat at absorber temperatures up to 175 °C, which is 27 °C higher than the temperature achieved with the SSHT.

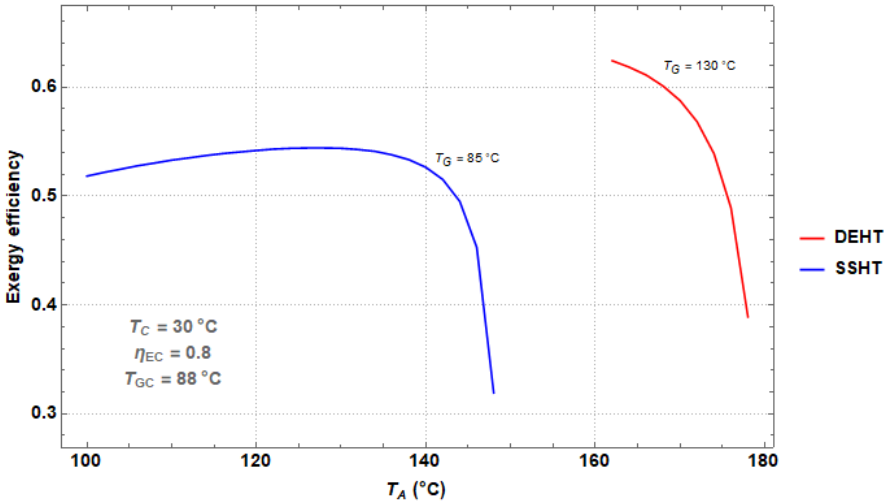

Figure 12. Comparison of the exergy efficiency as a function of T_A for the two different heat transformers.

5. Conclusions

A new configuration system called double-effect heat transformer operating with water/LiBr has been analyzed and then compared with the SSHT. The comparison was presented as a function of the main operating system parameters.

The results showed that the COP of the DEHT significantly decreased with the increment of the absorber temperature, the FR and the GTL, while increased with the increment of the generator temperature. The COP values did not present a significant change with the condenser temperature. The maximum COP value was 0.63, and the minimum was 0.31, while the GTL varied from 24 °C to 48 °C depending on the system operating temperatures and the heat exchanger effectiveness. The exergy values for the DEHT varied from 0.39–0.63.

From the comparison between the DEHT and the SSHT, it was observed that the proposed system was able to achieve COP values up to 25.8% higher than those obtained with the SSHT, but reaching lower GTL values.

From the analysis carried out, it can be stated that the proposed system is able to achieve the highest COP among all the heat transformer configurations reported in the literature.

Author Contributions: I.N.B.-S.: modeled the heat transformer configuration, analyzed the results and wrote part of the manuscript; J.C.J.-G. proposed part of the mathematical model and wrote part of the manuscript; W.R. proposed the original idea, analyzed the results and wrote part of the manuscript.

Conflicts of Interest: The authors declare no conflict of interest.

Nomenclature

AHT	Absorption Heat Transformer
COP	Coefficient of Performance (dimensionless)
DAHT	Double Absorption Heat Transformers
DEHT	Double Effect Heat Transformer
FR	Flow Ratio
GTL	Gross Temperature Lift (°C)
h	Specific enthalpy $\left(\frac{kJ}{kg}\right)$
HT	Heat Transformer
$\dot{m}$	Mass flow rate $\left(\frac{kg}{s}\right)$
η	Effectiveness (dimensionless)
ORC	Organic Rankine Cycle
P	Pressure (bar)
$\dot{Q}$	Thermal power (kW)
q	Vapor quality (dimensionless)
SSHT	Single-Stage Heat Transformer
T	Temperature (°C)
$\dot{W}$	Mechanical power (kW)
x	LiBr concentration (dimensionless)

Subscripts

A	absorber
C	condenser
E	evaporator
EC	economizer
G	generator
GC	generator-condenser
P	pump

References

1. Parham, K.; Khamooshi, M.; Tematio, D.B.K.; Yari, M.; Atikol, U. Absorption heat transformers—A comprehensive review. *Renew. Sustain. Energy Rev.* **2014**, *34*, 430–452. [CrossRef]
2. Donnellan, P.; Cronin, K.; Byrne, E. Recycling waste heat energy using vapour absorption heat transformers: A review. *Renew. Sustain. Energy Rev.* **2015**, *42*, 1290–1304. [CrossRef]
3. Rivera, W.; Best, R.; Cardoso, M.J.; Romero, R.J. A review of absorption heat transformers. *Appl. Therm. Eng.* **2015**, *91*, 654–670. [CrossRef]
4. Rivera, W.; Best, R.; Hernández, J.; Heard, C.L.; Holland, F.A. Thermodynamic study of advanced absorption heat transformers-I. Single and two stage configurations with heat exchangers. *Heat Recovery Syst. CHP* **1994**, *14*, 173–183. [CrossRef]
5. Rivera, W.; Best, R.; Hernández, J.; Heard, C.L.; Holland, F.A. Thermodynamic study of advanced absorption heat transformers-II. Double absorption configurations. *Heat Recovery Syst. CHP* **1994**, *14*, 185–193. [CrossRef]
6. Ji, J.; Ishida, M. Behavior of a two-stage absorption heat transformer combining latent and sensible heat exchange modes. *Appl. Energy* **1999**, *62*, 267–281. [CrossRef]
7. Göktun, S.; Er, I.D. Performance analysis of an irreversible cascaded heat-transformer. *Appl. Energy* **2002**, *72*, 529–539. [CrossRef]
8. Zhao, Z.; Ma, Y.; Chen, J. Thermodynamic performance of a new type of double absorption heat transformer. *Appl. Therm. Eng.* **2003**, *23*, 2407–2414. [CrossRef]
9. Zhao, Z.; Zhou, F.; Zhang, X.; Li, S. The thermodynamic performance of a new solution cycle in double absorption heat transformer using water/lithium bromide as the working fluids. *Int. J. Refrig.* **2003**, *26*, 315–320. [CrossRef]

10. Rivera, W.; Cardoso, M.J.; Romero, R.J. Single-stage and advanced absorption heat transformers operating with lithium bromide mixtures used to increase solar pond's temperature. *Sol. Energy Mater. Sol. Cells* **2001**, *70*, 321–333. [CrossRef]
11. Lee, S.F.; Sherif, S.A. *Second Law Analysis of Multi-Stage Lithium Bromide/Water Absorption Heat Transformers*; University of Florida: Gainesville, FL, USA, 2000.
12. Donnellan, P.; Byrne, E.; Cronin, K. Internal energy and exergy recovery in high temperature application absorption heat transformers. *Appl. Therm. Eng.* **2013**, *56*, 1–10. [CrossRef]
13. Donnellan, P.; Byrne, E.; Oliveira, J.; Cronin, K. First and second law multidimensional analysis of a triple absorption heat transformer (TAHT). *Appl. Energy* **2014**, *113*, 141–151. [CrossRef]
14. Fartaj, S.A. Comparison of energy, exergy, and entropy balance methods for analysing double-stage absorption heat transformer cycles. *Int. J. Energy Res.* **2004**, *28*, 1219–1230. [CrossRef]
15. Martínez, H.; Rivera, W. Energy and exergy analysis of a double absorption heat transformer operating with water/lithium bromide. *Int. J. Energy Res.* **2009**, *33*, 662–674. [CrossRef]
16. Wang, H.; Li, H.; Bu, X.; Wang, L. Effects of the generator and evaporator temperature differences on a double absorption heat transformer—Different control strategies on utilizing heat sources. *Energy Convers. Manag.* **2017**, *138*, 12–21. [CrossRef]
17. Wang, L.; Li, H.; Bu, X.; Wang, H.; Ma, W. Performance Study of a Double Absorption Heat Transformer. *Energy Procedia* **2017**, *105*, 1473–1482. [CrossRef]
18. Liu, F.; Sui, J.; Liu, H.; Jin, H. Experimental studies on a direct-steam-generation absorption heat transformer built with vertical falling-film heat exchangers. *Exp. Therm. Fluid Sci.* **2017**, *83*, 9–18. [CrossRef]
19. Salehi, S.; Yari, M.; Mahmoudi, S.M.S.; Farshi, L.G. Investigation of Crystallization Risk in Different Types of Absorption LiBr/H_2O Heat Transformers. *Therm. Sci. Eng. Prog.* **2019**, *10*, 48–58. [CrossRef]
20. Hernández-Magallanes, J.A.; Heard, C.L.; Best, R.; Rivera, W. Modeling of a new absorption heat pump-transformer used to produce heat and power simultaneously. *Energy* **2018**, *165*, 112–133. [CrossRef]
21. Rivera, W.; Cerezo, J.; Martínez, H. Energy and exergy analysis of an experimental single-stage heat transformer operating with the water-lithium bromide mixture. *Int. J. Energy Res.* **2010**, *34*, 1121–1131. [CrossRef]
22. Colorado, D.; Hernández, J.A.; Rivera, W.; Martínez, H.; Juárez, D. Optimal operation conditions for a single-stage heat transformer by means of an artificial neural network inverse. *Appl. Energy* **2011**, *88*, 1281–1290. [CrossRef]
23. Rivera, W.; Martínez, H.; Cerezo, J.; Romero, R.J.; Cardoso, M.J. Exergy analysis of an experimental single-stage heat transformer operating with single water/lithium bromide and using additives (1-octanol and 2-ethyl-1-hexanol). *Appl. Energy* **2011**, *31*, 3526–3532. [CrossRef]
24. Olarte Cortés, J.; Torres Merino, J.; Siqueiros, J. Experimental study of a graphite disks absorber couple to a heat transformer. *Exp. Therm. Fluid Sci.* **2013**, *46*, 29–36. [CrossRef]
25. Márquez Nolasco, A.; Delgado Gonzaga, J.; Huicochea, A.; Torres Merino, J.; Siqueiros, J.; Hernández, J.A. Experimental study of a graphite disk generator into an absorption heat transformer. *Appl. Therm. Eng.* **2018**, *143*, 849–858. [CrossRef]
26. Ma, X.H.; Lan, Z.; Hao, Z.; Wang, Q.C.; Bo, S.; Bai, T. Heat transfer and thermodynamic performance of LiBr/H_2O absorption heat transformer with vapor absorption inside vertical spiral tubes. *Heat Transf. Eng.* **2014**, *35*, 1130–1136. [CrossRef]
27. Hong, S.J.; Lee, C.H.; Kim, S.M.; Kim, I.G.; Kwon, O.K.; Park, C.W. Analysis of single stage steam generating absorption heat transformer. *Appl. Therm. Eng.* **2018**, *144*, 1109–1116. [CrossRef]
28. Conde Gutiérrez, R.A.; Cruz Jacobo, U.; Huicochea, A.; Casolco, S.R.; Hernández, J.A. Optimal multivariable conditions in the operation of an absorption heat transformer with energy recycling solved by the genetic algorithm in artificial neural network inverse. *Appl. Soft Comput.* **2018**, *72*, 218–234. [CrossRef]
29. Ibarra Bahena, J.; Romero, R.J.; Velázquez-Avelar, L.; Valdez Morales, C.V.; Galindo Luna, Y.R. Evaluation of the thermodynamic effectiveness of a plate heat exchanger integrated into a experimental single stage heat transformer operating with water/Carrol mixture. *Exp. Therm. Fluid Sci.* **2013**, *51*, 257–263. [CrossRef]